

Influence of Metal Cations on the Intramolecular Hydrogen-Bonding Network and pK_a in Phosphorylated Compounds

Ping Yang,^{*,†,§} Bernard Spiess,[‡] Pushpalatha P. N. Murthy,[§] and Richard E. Brown^{*,§}

Theoretical Division, MS B268, Los Alamos National Laboratory, Los Alamos, New Mexico 87544, Laboratoire de Pharmacochimie Moléculaire, UPR 421 du CNRS, Faculté de Pharmacie, 74, route du Rhin, B.P. 24, 67401 Illkirch Cedex, France, and Department of Chemistry, Michigan Technological University, Houghton, Michigan 49931

Received: December 22, 2006; In Final Form: February 15, 2007

The binding of the most common metal cations of cytoplasm (Li^+ , Na^+ , K^+ , Mg^{2+} and Ca^{2+}) to a model molecule having an intramolecular hydrogen-bonding network, *myo*-inositol-2-monophosphate, was studied using first principles. A strong correlation between the conformation of metal inositol phosphate complexes with the type of metal cation, degree of deprotonation state, and the surrounding environment has been observed. On the basis of the hydrogen-bonding network analysis of the cation-phosphate complexes ($\text{M}^{n+}-\text{Ins}(2)\text{P}_1$), the alkali cations show little effect on the conformational preference while the conformational preference for the binding of the alkaline earth cations is pH-dependent and solvent-dependent. For example, these calculations predict that $\text{Mg}^{2+}-\text{Ins}(2)\text{P}_1^0$ and $\text{Mg}^{2+}-\text{Ins}(2)\text{P}_1^{2-}$ favor the 1a/5e form while $\text{Mg}^{2+}-\text{Ins}(2)\text{P}_1^{1-}$ favors the 5a/1e conformation. The $\text{Ca}^{2+}-\text{Ins}(2)\text{P}_1^{2-}$ complex prefers the 1a/5e conformation in the gas phase and in a nonpolar protein environment, but inverts to the 5a/1e conformation upon entering the polar aqueous phase. The binding affinities of the cations and the pK_a values for the cation-phosphate complexes are derived from thermodynamical analysis.

Introduction

Within natural biological systems, there exist important metal cations such as the monovalent alkali cations (Li^+ , Na^+ , K^+) and the divalent alkaline earth metal cations (Mg^{2+} and Ca^{2+}).¹ All of these Lewis acidic metal centers are chemically well-suited to influence fundamental cellular processes and play vital bio-functional roles within and outside the cell such as triggering cellular responses and being involved in cell metabolism^{2,3} due to their different affinities and interactions with basic nitrogen or oxygen donor ligands. Metal ions, as a common feature in folding of proteins, DNA, and RNA, have a special relationship with the phosphate group, PO_4^{3-} , to stabilize nucleic acids by mediating electrostatic repulsion between negatively charged phosphates.^{4,5} Particularly appealing is that these cations affect the intramolecular hydrogen-bonding network and cause conformational changes that can provide new methods for studying DNA and RNA.⁶ The functions of the second messenger and the phosphalated membrane structures are not clear at the molecular level. In biological systems, the phosphate group is usually not isolated as a functional group of a large molecule. Accordingly, the phosphate group is often involved in an intramolecular or intermolecular hydrogen-bonding network (HBN). Experimental data show that cations directly contact oxygen atoms in the phosphate moiety, especially when they are buried inside a protein.^{7,8} Not much is known about the binding strength of different metal ions to such phosphate groups within hydrogen-bonding networks and the reorganization of hydrogen bonds caused by electrostatic interactions. Nevertheless, there is no systematic investigation into the interactions

between cations and phosphate groups and hydrogen-bonding network within biological systems.

Furthermore, to understand the chemistry and structures of metal cations interacting with phosphate groups and a hydrogen-bonding network, a rule of thumb is to study those motifs provided by nature in existing systems. In this paper, we report the fundamental interactions and binding strengths between HBN and metal cations via a phosphate group. We choose a model system, $\text{Ins}(2)\text{P}_1$, which includes the fundamental structural features of such systems in order to explore the effect of cations on the hydrogen-bonding network between the phosphate group and hydroxyl groups. We have observed and quantitatively analyzed a strong correlation between conformation and the degree of deprotonation for *myo*-inositol 2-monophosphate ($\text{Ins}(2)\text{P}_1$),⁹ shown in Figure 1. It is one of the important participants in the role that phosphates play in biological and environmental chemistry.³ This model system allows us to investigate the hydrogen bonding and other electrostatic interactions between these functional groups and metal ions at every state of deprotonation. The intramolecular hydrogen-bonding and the interactions with cations are critical to many biological functions. The results from our model systems will help to guide accurate simulations of proteins, RNAs and membrane structures that interact with cations at different pH.

The understanding of the coupling between metal cations and the phosphate group within HBN can help decipher the biological mechanisms involving these species. For example, Li^+ can produce a lowering of *myo*-inositol concentration in critical areas of the brain by interacting with the substrate, inositol monophosphate, of *myo*-inositol monophosphatase (IMP) and result in the inositol depletion hypothesis for bipolar disorder.^{8,10} There is still much controversy surrounding the issue about the competition between Li^+ and Mg^{2+} in the proposed

* Corresponding authors. E-mails: pyang@lanl.gov, rebrown@mtu.edu.

† Los Alamos National Laboratory.

‡ Laboratoire de Pharmacochimie Moléculaire.

§ Michigan Technological University.

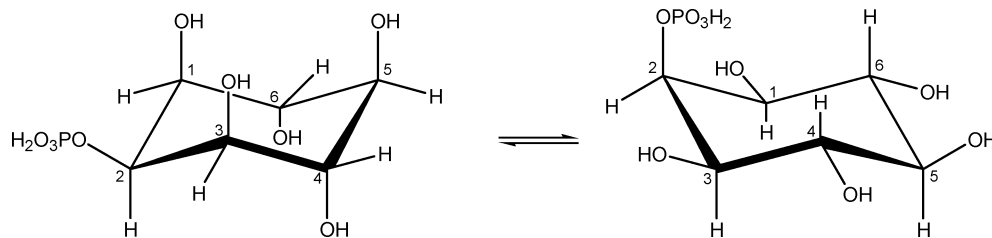


Figure 1. *myo*-Inositol 2-monophosphate (Ins(2)P₁) can adopt two chair conformations. One conformation, on right, is with the phosphate group in the axial position and the five hydroxyl groups in equatorial position (1a/5e). The other conformation, on left, is with the phosphate group in equatorial while the five hydroxyl groups are axial (5a/1e).

mechanisms for the pharmacological action of lithium salts in bipolar disorder.¹¹ *myo*-Inositol phosphates and inositol phospholipids play an essential role in signal transduction in biological systems via mediating Ca²⁺ homeostasis.^{12,13} Ca²⁺, which is required for the activity of phospholipase C, interacts with negatively charged residues and with phosphate moieties of the phosphorylated inositol at the active sites. Magnesium and calcium are the most versatile metal cofactors in cellular biochemistry, playing both intracellular and extracellular roles. For example, Mg²⁺ and Ca²⁺ have been recruited to cleave the phosphodiester linkages due in part to their ability to lower the pK_a of coordinated water, creating the active hydroxyl nucleophile. Additionally, Mg²⁺ and Ca²⁺ also function in biological membranes to neutralize charge on phosphorylated head-groups of lipids.

First-principles studies provide a valuable tool for understanding the structural constraints and functional attributes of these metal ions complexes. The aim of our work is to gain insight into the metal ion-carrier interactions through theoretical modeling. As a prototype for studying the cation-coordinated complexes, we examined the structures and binding affinities of complexes of Ins(2)P₁ with metal cations. Our attention is focused on the following aspects: (1) how do different metal cations change the structure/hydrogen-bonding network of *myo*-inositol monophosphate, (2) what is the relative binding strength of the alkali/alkaline-earth cations to Ins(2)P₁, (3) what is the pH-dependence of metal ions complexes, i.e., for each cation what are the differences and similarities of their interactions with the different deprotonation states, (Mⁿ⁺–Ins(2)P₁⁰, Mⁿ⁺–Ins(2)P₁¹⁻, Mⁿ⁺–Ins(2)P₁²⁻), (4) what are the solvation effects including nonpolar and polar solvents, and (5) how do different cations affect the pK_a?

Computational Methods

Density functional theory is now commonly applied to biological systems, as it has been shown to reliably reproduce experimental data at a reasonable computational cost.¹⁴ The Becke three-parameter hybrid functional combined with the Lee, Yang, and Parr correlation functional, (B3LYP),^{15–18} was employed in this work. The calculations were carried out using the 6-31+G(d) basis sets which includes diffuse and polarization functions. In previous work on similar systems, the basis set superposition errors (BSSE) were found to be small and were omitted here.^{18–20} Harmonic vibrational analyses were performed at the same level to confirm that each structure was a minimum on the potential energy surface and to determine the enthalpy and free energy of each structure.²¹ The vibrational analyses were carried out on all optimized structures to get the thermo-chemical contributions to the energy and entropy from the vibrational, rotational and translational degrees of freedom at standard state conditions, i.e., 298.15 K and 1 atm.

For Ins(2)P₁, there are two possible chair conformations, i.e., the 1a/5e and 5a/1e conformations, as shown in Figure 1. From

previous work,⁹ the dominate species in both the gaseous and aqueous phases assumed the 1a/5e conformation for all degrees of deprotonation, Ins(2)P₁⁰, Ins(2)P₁¹⁻ and Ins(2)P₁²⁻. In this work, these studies are extended to include the complexes formed between these species and the most common metal cations of cytoplasm, Li⁺, Na⁺, K⁺, Mg²⁺, and Ca²⁺. In this current work, we only consider the directly bounded complexes without including the solvation shells of the cations. As a consequence, we do not discuss the complexes that have water molecules or other solvent molecules bridging the cations and the inositol monophosphates.

In order to clarify the various species discussed in this work, we use the following notation. We use the notation ^mOH to refer to the hydroxyl group at position *m* on the ring. The accepted ring numbering system is given in Figure 1. For example, ¹OH means the hydroxyl group on carbon 1 of inositol ring. The effect of cations on the relative stability between these two conformations (1a/5e and 5a/1e) was investigated in terms of their relative energy. We use the notation, Ins(2)P⁰(1a/5e), to refer the 1a/5e conformation of the neutral species Ins(2)P⁰ and Ins(2)P¹⁻(5a/1e) for the 5a/1e conformation of the partially deprotonated form Ins(2)P¹⁻. The notation, Mⁿ⁺–Ins(2)P₁⁰(5a/1e), will be used to refer to both the alkali and alkaline earth cation complexes with the 5a/1e conformation of the neutral species Ins(2)P⁰, where M is an alkali cation (Li⁺ or Na⁺ or K⁺) when *n* equals to 1 and an alkaline earth cation (Mg²⁺ or Ca²⁺) when *n* equals to 2.

The binding energies for these complexes in both conformations have been computed via the following equation. The interaction energies (i.e., the binding energies) of the metal cations with the *myo*-inositol monophosphate are calculated as the energy difference between the free energy of the optimized cation-monophosphate complex and those of the cation and the optimized monophosphate:

$$BE = E_{(M^{n+}-Ins(2)P_1)} - E_{(Ins(2)P_1)} - E_{(M^{n+})}$$

BE is the binding energy for each cation

$E_{(M^{n+}-Ins(2)P_1)}$ is the energy of a complex of Ins(2)P₁ and a cation

$E_{(M^{n+})}$ is the energy of the cation

$E_{(Ins(2)P_1)}$ is the energy of Ins(2)P₁

The *myo*-inositol phosphates easily dissolve in water due to the existence of hydroxyl and phosphate groups. The reactions of the *myo*-inositol phosphates usually happen on the surface or buried within the protein, and the chair-to-chair inversion for some members has been observed experimentally under aqueous environment.^{22,23} Thus, how the solvent affects the conformation is an important issue to clarify. In our calculations,

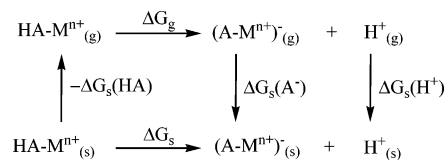


Figure 2. Thermodynamic cycle used to evaluate $\text{p}K_{\text{a}}$ values by absolute method.

we studied the solvation effects by using the polarized continuum model (PCM), which was developed by Tomasi and co-workers.^{24–28} Recent studies show that the implicit solvent model provides reasonable agreement with the experimental observables for systems involving intramolecular hydrogen bonds between hydroxyl and phosphate groups.^{9,29,30} We restricted our solvent phase calculations in this report to the optimized geometries in the gas phase because we are investigating the direct binding interactions between cations and the phosphate group within a hydrogen-bonding network. Especially when complexes are buried within a protein, the geometries usually do not have much flexibility. In this case, the possible best way to understand the solvation effects is to simulate the solvent as a surrounding continuous medium with a certain dielectric constant. In addition, the geometry optimizations for these charged complexes entail convergence problems using the implicit model, which is not surprising due to the subtle electrostatic interactions between the charged groups with the solvent medium. But the implicit solvent model can offer some understanding of how solvation effects the binding energies for those directly bound complexes in protein and water. We need to point out that the equilibrium position of the metal cation is sensitive to the environment. These binding energies might be different from those for the fully optimized solvated geometries. An additional step could be to use explicit solvent molecules for first solvation shell and to do ab initio molecular dynamics, which can simulate the hydrogen bonds and coordination interactions with good accuracy. This research is currently in progress.

A dielectric constant of 78.39 was used to represent water media, and a dielectric constant of 4.9 (chloroform) was used as a representative value for protein interiors.³¹ It has been shown that the free energy of solvation can be accurately computed also using the in-vacuo optimized geometry at the same level of theory.^{26,32–34} For the SCRF method, the radius of each atom in the molecule was calculated using the united atom topological model.^{35,36} For the two possible thermally accessible conformations (1a/5e and 5a/1e), we investigated the influence of these cations by fully optimizing each complex of $\text{Ins}(2)\text{P}_1^0$, $\text{Ins}(2)\text{P}_1^{1-}$, and $\text{Ins}(2)\text{P}_1^{2-}$ with the cations (Li^+ , Na^+ , K^+ , Mg^{2+} , Ca^{2+}) at the B3LYP/6-31+G(d) level. All calculations were carried out with the Gaussian 2003 program suite.³⁷

Cations could significantly affect the absolute $\text{p}K_{\text{a}}$ values of acids by balancing the negative charge and changing the conformation. Our calculations follow the thermodynamic cycle shown in Figure 2: the solute molecule (acid) is taken out of solution and dissociated in a vacuum and then the fragments are finally reinserted into solution. In our calculation, the value of $\Delta G_{\text{s}}^{\circ}(\text{H}^+) = -264.0$ kcal/mol is used to obtain the $\text{p}K_{\text{a}}$ for complexes of $\text{Ins}(2)\text{P}_1$ with metal cations.⁹

The free energy of dissociation in solution can be decomposed into the corresponding free energy for the reaction in the gas-phase, ΔG_{g} , and the sum of the free energies of solvation for each species

$$\begin{aligned}
 \Delta G_{\text{s}}^{\circ} &= G^{\circ}((\text{A} - \text{M}^{n+})_{\text{s}}^{-}) + G^{\circ}(\text{H}_{\text{s}}^{+}) - G^{\circ}((\text{HA} - \text{M}^{n+})_{\text{s}}) \\
 &= \Delta G_{\text{g}}^{\circ} + \Delta G_{\text{s}}^{\circ}(\text{A} - \text{M}^{n+})_{\text{s}}^{-} + \Delta G_{\text{s}}^{\circ}(\text{H}^+) - \Delta G_{\text{s}}^{\circ}(\text{HA} - \text{M}^{n+})_{\text{s}} \\
 &= \Delta G_{\text{g}} + \Delta \Delta G_{\text{s}}
 \end{aligned}$$

where, $n = 1$, M^{n+} is Li^+ , Na^+ , and K^+ ; $n = 2$, M^{n+} is Mg^{2+} and Ca^{2+} .

$$\Delta G_{\text{g}} = G^{\circ}((\text{A} - \text{M}^{n+})_{\text{g}}^{-}) + G^{\circ}(\text{H}_{\text{g}}^{+}) - G^{\circ}((\text{HA} - \text{M}^{n+})_{\text{g}})$$

$$\Delta \Delta G_{\text{s}} = \Delta G_{\text{s}}^{\circ}(\text{A} - \text{M}^{n+})_{\text{s}}^{-} + \Delta G_{\text{s}}^{\circ}(\text{H}^+) - \Delta G_{\text{s}}^{\circ}(\text{HA} - \text{M}^{n+})_{\text{s}}$$

Given the dissociation free energy in water, the $\text{p}K_{\text{a}}$ of the metal cation complexes can be calculated by using the following equation:

$$\text{p}K_{\text{a}} = \Delta G_{\text{g}}^{\circ}/2.303RT$$

Results and Discussion

1. Gas-Phase Geometries of the M^{n+} - $\text{Ins}(2)\text{P}_1$ Complexes.

The geometrical parameters for the optimized structures of the neutral and deprotonated forms of $\text{Ins}(2)\text{P}_1$ as well as their complexes with the alkali and alkaline earth cations are listed in Table 1.

1.1. M^{n+} - $\text{Ins}(2)\text{P}_1^0$. The 1a/5e conformation of $\text{Ins}(2)\text{P}_1^0$ forms a unidirectional hydrogen-bonding network (HBN) within the molecule to take advantage of hydrogen-bonding cooperativity. When this neutral structure interacts with the monovalent cations: Li^+ , Na^+ , and K^+ , the dominate interaction is the electrostatic attraction between the positively charged cation and the partially negatively charged oxygen atom in phosphoric acid group. These alkali cations bind in a monodentate fashion and do not affect the hydrogen-bonding network formed within the 1a/5e conformation of $\text{Ins}(2)\text{P}_1^0$. The binding distances between the cations and oxygen atom in the phosphoric acid group are 1.728, 2.098, and 2.485 Å for Li^+ , Na^+ , and K^+ respectively. The smaller cation binds to $\text{Ins}(s)\text{P}_1^0$ more tightly due to the smaller ionic radii of the metal cations, (Li^+ 0.60 Å, Na^+ 0.95 Å, K^+ 1.33 Å, Mg^{2+} 0.65 Å, Ca^{2+} 0.99 Å). Compared to the monovalent alkali metal ions, the divalent alkaline earth cations Mg^{2+} and Ca^{2+} bind to $\text{Ins}(2)\text{P}_1^0(1a/5e)$ multidentately and induce much larger conformational changes. They can form tridentate bonds with the oxygen atoms of the hydroxyl groups on the 1 and 6 positions (^1OH and ^6OH) and the phosphoric acid group at the 2-position. Phosphate ligands exhibit Ca–O internuclear distances that range between 2.26 and 2.39 Å, while Mg–O distances range from 1.91 to 2.02 Å.

Therefore, the intramolecular hydrogen-bonding network (intra-HBN) is disrupted by the cations via breaking the hydrogen bond between ^6OH and ^1OH and the one between the phosphate group and ^1OH , although a relatively stronger hydrogen bond between ^6OH and ^5OH is formed. Due to the strong interactions with the divalent cations, the three hydrogen bonds involving the ^3OH and ^4OH groups opposite the cations are significantly stretched and weakened. The cooperativity of the intra-HBN is diminished due to the breakup of the unidirectional hydrogen bonding interactions.

Generally speaking, the interactions with the metal cations lead to a much larger conformational change in the 5a/1e conformation than in the 1a/5e conformation. The intra-HBN is destroyed in the M^{n+} - $\text{Ins}(2)\text{P}_1^0(5a/1e)$ complexes. Multidentate cation-oxygen coordination bonds are formed even for

TABLE 1: Conformations of *Myo*-Inositol 2-Monophosphate and Its Anions with Cations^a

		Li ⁺	Na ⁺
Ins(2)P ₁ ⁰ (1a/5e)			
Ins(2)P ₁ ⁰ (5a/1e)			
Ins(2)P ₁ ¹⁻ (1a/5e)			
Ins(2)P ₁ ¹⁻ (5a/1e)			
Ins(2)P ₁ ²⁻ (1a/5e)			
Ins(2)P ₁ ²⁻ (5a/1e)			

TABLE 1: (Continued)

	K^+	Mg^{2+}	Ca^{2+}
$Ins(2)P_1^0$ (1a/5e)			
$Ins(2)P_1^0$ (5a/1e)			
$Ins(2)P_1^{1-}$ (1a/5e)			
$Ins(2)P_1^{1-}$ (5a/1e)			
$Ins(2)P_1^{2-}$ (1a/5e)			
$Ins(2)P_1^{2-}$ (5a/1e)			

^a P, O, C, and H atoms are gold, red, gray, and white, respectively. Alkali (alkaline earth) cations are purple (green). The hydrogen bond lengths are blue and coordination bond lengths are green. The stretched OH bonds are shown in pink.

the monovalent cations Li^+ , Na^+ , and K^+ due to the accessible distances to the oxygen atoms of the phosphate group and the ^1OH , ^3OH groups. Both Li^+ and Na^+ form tridentate coordination bonds with these oxygen atoms, which are about 0.3 Å longer than the monodentate coordinating bonds in the 1a/5e complexes. In a similar fashion, the alkaline earth metal cations, Mg^{2+} and Ca^{2+} , bind to the $\text{Ins}(2)\text{P}_1^0(5a/1e)$ forming multidentate coordination bonds with average lengths of 2.04 Å and 2.41 Å.

1.2. $M^{n+}-\text{Ins}(2)\text{P}_1^{1-}$. As opposed to the $M^{n+}-\text{Ins}(2)\text{P}_1^0(1a/5e)$ complexes, all metal ions including the alkali metal and alkaline earth cations are tridentately coordinated with one oxygen atom from the ^1OH group and two oxygen atoms from the phosphate group including the phosphoester oxygen. The unidirectional intra-HBN in $\text{Ins}(2)\text{P}_1^{1-}(1a/5e)$ is conserved in each metal cation complex for the reason that the metal cations are trapped more locally to the phosphate group with the increase of the negative charge. With higher charge on the phosphate group, less involvement of the hydroxyl groups is needed to compensate the charge on the metal cations. Increasing the radius of the metal cations enhances the intra-HBN. For example, the shortest hydrogen bond between the phosphate group and ^3OH in the intra-HBN is 2.069, 1.837, and 1.738 Å corresponding to the Li^+ , Na^+ , and K^+ complexes, compared to 2.360 and 1.936 Å for Mg^{2+} and Ca^{2+} . A larger metal cation leads to a stronger intra-HBN since a longer coordination bond length imposes less stress when forming multiple coordination bonds. The coordination bond lengths for Mg^{2+} and Ca^{2+} are slightly shorter than those within the neutral complexes, due to the larger negative charge on the phosphate group and resulting stronger electrostatic interactions with the cations.

To form the $M^+-\text{Ins}(2)\text{P}_1^{1-}(5a/1e)$ complexes, the binding pattern for Li^+ is very similar to that for Na^+ and K^+ with the same tridentate configuration as in the $M^+-\text{Ins}(2)\text{P}_1^{1-}(1a/5e)$ complexes. However, the coordination bond distances are different. The original intra-HNB is partially perturbed in order to form the cation-oxygen coordination bonds. The intra-HBN of $\text{Ins}(2)\text{P}_1^{1-}$ is again diminished in the metalated complexes. The same hydrogen bonds among ^1OH , ^5OH and ^3OH groups are formed in all alkali cation complexes. The coordination bonds become longer with increasing cation radii. Mg^{2+} and Ca^{2+} form one more coordination bond in $M^{2+}-\text{Ins}(2)\text{P}_1^{1-}(5a/1e)$ than in $M^{2+}-\text{Ins}(2)\text{P}_1^{1-}(1a/5e)$, in a fashion similar to the complexes of the alkaline earth cations with $\text{Ins}(2)\text{P}_1^0(5a/1e)$. These coordination bonds have lengths similar to those in the 1a/5e complexes and are somewhat shorter than those formed in the complexes with the neutral complexes, $M^{2+}-\text{Ins}(1)\text{P}_1^0(5a/1e)$. Therefore, the complexes of the alkaline earth cations have higher binding affinities for the 5a/1e conformation than for the 1a/5e conformation of $\text{Ins}(2)\text{P}_1^{1-}$.

1.3. $M^{n+}-\text{Ins}(2)\text{P}_1^{2-}$. The intra-HBN is mostly conserved in the complexes of $M^+-\text{Ins}(2)\text{P}_1^{2-}(1a/5e)$. The hydrogen bond between the phosphate and ^1OH groups is significantly shortened within the complexes of $M^+-\text{Ins}(2)\text{P}_1^{2-}(1a/5e)$ compared to the bare molecule $\text{Ins}(2)\text{P}_1^{2-}(1a/5e)$. At same time, the lengthening of the ^1OH bond decreases from Li^+ to Na^+ to K^+ . Due to the two short bonds formed between Li^+ and the phosphate oxygen and the ^1OH oxygen with lengths of 1.78 Å and 1.79 Å respectively, the proton transfer from ^1OH to the phosphate group proceeds without an energy barrier within $\text{Li}^+-\text{Ins}(2)\text{P}_1^{2-}(1a/5e)$. The ^1OH bond is stretched to 1.037 Å in the $\text{Na}^+-\text{Ins}(2)\text{P}_1^{2-}$ complex with the hydrogen bond length of 1.558 Å, while the ^1OH bond is stretched to 1.033 Å in the $\text{K}^+-\text{Ins}(2)\text{P}_1^{2-}$ complex with a hydrogen bond length of 1.573 Å. It seems

fair to say that alkali cations could assist the intramolecular proton transfer. The binding pattern of Mg^{2+} and Ca^{2+} are similar in terms of forming multidentate coordination bonds and decreasing the stretched ^1OH bond back to a normal length resulting in a longer hydrogen bond. Similarly, due to the localization of metal cations to the phosphate group, the hydrogen-bonding network is more similar to that for bare $\text{Ins}(2)\text{P}_1^{2-}(1a/5e)$.

The intra-HBN is mostly left intact with a small conformational change in the complexes of $M^+-\text{Ins}(2)\text{P}_1^{2-}(5a/1e)$ due to the localization of alkali cations on the fully charged phosphate group. Alkali cations bind to the phosphate group only bidentately. Thus the charges at the metal cations are locally neutralized by the phosphate group. Consequently, the hydrogen-bonding network of the 5a/1e conformation of $\text{Ins}(2)\text{P}_1^{2-}$ is conserved in these complexes. Because of the charge compensation from the alkali cations, the hydrogen bond between the phosphate group and ^3OH is considerably weakened giving a normal hydroxyl bond for ^3OH within the complexes of $M^+-\text{Ins}(2)\text{P}_1^{2-}(5a/1e)$. For Mg^{2+} and Ca^{2+} , both the 1a/5e and 5a/1e conformations form tetradentately bonded complexes. Significant interactions occur between the cations and the phosphoester oxygen atom, the phosphorus atom, the ^1OH oxygen atom and the two O^- atoms on the phosphate group. The higher the charge on the phosphate group, the more the cations are localized near the phosphate group resulting in less interaction of the cations with the rest of the intra-HBN. Within the complexes with the 5a/1e conformation, the alkaline earth cations enhance the intramolecular hydrogen bonding interaction to form fairly short hydrogen bonds of 1.594 and 1.582 Å. This significantly lowers the system energy and possibly causes the complex to be more stable than for the corresponding 1a/5e complex.

2. Energetics of the $M^{n+}-\text{Ins}(2)\text{P}_1$ Complexes. The gas-phase binding energies, zero-point energy (ZPE) corrections and Gibbs free energies of $M^{n+}-\text{Ins}(2)\text{P}_1$ are summarized in Table 2. The binding affinities and Gibbs free energies in water and chloroform are also listed in Table 2 as well. Table 3 shows the relative stabilities of the 1a/5e and 5a/1e conformations for each $M^{n+}-\text{Ins}(2)\text{P}_1$ complex.

In general, for each conformation of $\text{Ins}(2)\text{P}_1$ at each deprotonation state, the binding energies with metal cations are ordered as $\text{Mg}^{2+} > \text{Ca}^{2+} > \text{Li}^+ > \text{Na}^+ > \text{K}^+$. The smaller cation binds to $\text{Ins}(2)\text{P}_1$ more tightly in terms of affinity strength. For each cation, these calculations predict that the binding energy increases with increasing charge on the phosphate group, i.e., the increase in the degree of deprotonation such that $\text{Ins}(2)\text{P}_1^{2-} > \text{Ins}(2)\text{P}_1^{1-} > \text{Ins}(2)\text{P}_1^0$. Essentially, electrostatic interactions dominate the binding in these systems. Smaller ions give shorter metal-ligand distances and generate greater ion-ion, ion-dipole and ion-induced dipole interactions.

2.1. $M^{n+}-\text{Ins}(2)\text{P}_1^0$. For the stable structures of the $M^+-\text{Ins}(2)\text{P}_1^0$ complexes, the dominant electrostatic interaction is between the cation and the partially negatively charged oxygen atoms of the phosphoric acid group. For the monovalent cations, Li^+ , Na^+ , and K^+ , the binding energies are -58.98, -43.98, and -32.49 kcal/mol, respectively, to form $M^+-\text{Ins}(2)\text{P}_1^0(1a/5e)$ in the gas phase, whereas the binding energies are -68.78, -47.54, and -33.85 kcal/mol for $M^+-\text{Ins}(2)\text{P}_1^0(5a/1e)$. Obviously, the cations actually bind to the 5a/1e conformation more strongly. For each chair conformation of $M^+-\text{Ins}(2)\text{P}_1^0$, the binding order is $\text{Li}^+ > \text{Na}^+ > \text{K}^+$. The binding affinities for Li^+ are about 39% higher than for Na^+ and those for Na^+ are

TABLE 2: Binding Energies of Myo-Inositol 2-Monophosphate and Its Anions with Cations (kcal/mol)^a

	metal cations	Li ⁺	Na ⁺	K ⁺	Mg ²⁺	Ca ²⁺
M ⁿ⁺ -Ins(2)P ₁ ⁰ (1a/5e)	$\Delta_g E_{BE}$	-58.98	-43.98	-32.49	-211.05	-141.10
	$\Delta_g E_{BE} + ZPE$	-57.86	-43.35	-32.10	-209.79	-140.25
	$\Delta_g G_{BE}$	-50.96	-36.34	-25.60	-200.26	-131.00
	$\Delta_w E_{BE}$	-16.42	-15.20	-13.71	-51.29	-23.11
	$\Delta_w G_{BE}$	-4.31	-2.77	-1.50	-38.37	-10.19
	$\Delta_c E_{BE}$	-24.08	-19.62	-15.69	-96.54	-54.64
	$\Delta_c G_{BE}$	-16.97	-12.27	-8.55	-88.26	-46.47
M ⁿ⁺ -Ins(2)P ₁ ⁰ (5a/1e)	$\Delta_g E_{BE}$	-68.78	-47.54	-33.85	-214.43	-141.35
	$\Delta_g E_{BE} + ZPE$	-67.85	-47.45	-33.70	-213.57	-140.82
	$\Delta_g G_{BE}$	-60.65	-41.28	-26.49	-204.76	-132.56
	$\Delta_w E_{BE}$	-19.80	-14.49	-15.37	-55.17	-26.41
	$\Delta_w G_{BE}$	-10.57	-3.98	-4.50	-45.07	-16.35
	$\Delta_c E_{BE}$	-27.79	-19.48	-17.04	-99.38	-56.32
	$\Delta_c G_{BE}$	-22.60	-13.64	-10.52	-93.13	-50.24
M ⁿ⁺ -Ins(2)P ₁ ¹⁻ (1a/5e)	$\Delta_g E_{BE}$	-151.72	-128.08	-111.10	-377.34	-295.74
	$\Delta_g E_{BE} + ZPE$	-149.51	-126.72	-109.91	-375.43	-294.07
	$\Delta_g G_{BE}$	-141.76	-118.80	-102.25	-366.97	-285.72
	$\Delta_w E_{BE}$	-22.25	-21.08	-19.55	-64.91	-33.49
	$\Delta_w G_{BE}$	-9.46	-8.08	-6.12	-51.48	-20.77
	$\Delta_c E_{BE}$	-51.79	-43.85	-38.77	-145.96	-98.28
	$\Delta_c G_{BE}$	-44.08	-36.07	-30.62	-137.67	-90.55
M ⁿ⁺ -Ins(2)P ₁ ¹⁻ (5a/1e)	$\Delta_g E_{BE}$	-154.04	-129.87	-107.36	-395.01	-300.17
	$\Delta_g E_{BE} + ZPE$	-152.19	-128.39	-106.23	-393.19	-299.38
	$\Delta_g G_{BE}$	-144.79	-119.79	-98.14	-383.88	-290.92
	$\Delta_w E_{BE}$	-21.41	-19.35	-18.21	-77.37	-40.27
	$\Delta_w G_{BE}$	-11.41	-6.98	-4.87	-66.00	-29.44
	$\Delta_c E_{BE}$	-53.03	-44.18	-37.06	-162.70	-105.05
	$\Delta_c G_{BE}$	-47.25	-36.55	-28.82	-155.71	-98.85
M ⁿ⁺ -Ins(2)P ₁ ²⁻ (1a/5e)	$\Delta_g E_{BE}$	-244.97	-209.62	-186.85	-562.46	-458.90
	$\Delta_g E_{BE} + ZPE$	-242.52	-208.80	-186.27	-560.22	-457.60
	$\Delta_g G_{BE}$	-235.13	-201.49	-179.33	-552.08	-449.66
	$\Delta_w E_{BE}$	-26.97	-23.51	-21.70	-78.90	-36.30
	$\Delta_w G_{BE}$	-14.13	-11.44	-9.57	-66.41	-24.51
	$\Delta_c E_{BE}$	-80.35	-65.53	-57.98	-206.48	-140.82
	$\Delta_c G_{BE}$	-72.44	-58.59	-50.96	-198.65	-133.69
M ⁿ⁺ -Ins(2)P ₁ ²⁻ (5a/1e)	$\Delta_g E_{BE}$	-241.35	-209.93	-185.15	-564.17	-473.31
	$\Delta_g E_{BE} + ZPE$	-237.68	-207.30	-182.99	-560.76	-470.19
	$\Delta_g G_{BE}$	-230.50	-199.91	-176.03	-551.82	-461.25
	$\Delta_w E_{BE}$	-29.51	-24.22	-18.92	-72.48	-37.06
	$\Delta_w G_{BE}$	-21.41	-16.45	-11.55	-63.90	-29.54
	$\Delta_c E_{BE}$	-83.44	-69.91	-59.40	-208.83	-153.51
	$\Delta_c G_{BE}$	-74.72	-61.58	-51.36	-199.28	-144.75

^a $\Delta_g E_{BE}$ is the binding energy in gas phase, and $\Delta_g E_{BE} + ZPE$ is the binding energy, including zero-point energy correction. $\Delta_g G_{BE}$ is the binding Gibbs free energy change in gas phase. The subscripts of w and c refer to the binding energy in water and CHCl₃, respectively.

TABLE 3: Energies Difference between ($E_{1a/5e} - E_{5a/1e}$) Conformation, with Effect of Cations (kcal/mol)^a

	cations	Ins(2)P ₁	Li ⁺	Na ⁺	K ⁺	Mg ²⁺	Ca ²⁺
Ins(2)P ₁ ⁰	$\Delta_g E$	-7.56	-3.00	-3.25	-5.44	-3.42	-6.56
	$\Delta_w E$	-8.11	-4.73	-8.81	-6.45	-4.23	-4.81
	$\Delta_c E$	-6.28	-2.57	-6.42	-4.93	-3.43	-4.60
Ins(2)P ₁ ¹⁻	$\Delta_g E$	-6.17	-2.98	-3.52	-9.05	12.36	-0.88
	$\Delta_w E$	-8.53	-9.37	-10.26	-9.86	3.93	-1.74
	$\Delta_c E$	-6.72	-5.48	-6.38	-8.43	10.02	0.05
Ins(2)P ₁ ²⁻	$\Delta_g E$	-4.56	-8.54	-4.60	-6.61	-3.21	9.49
	$\Delta_w E$	-7.53	-5.00	-6.82	-10.31	-13.95	-6.77
	$\Delta_c E$	-8.92	-5.83	-4.55	-7.51	-6.58	3.77

^a The same notation is used as in Table 2.

about 37% higher than for K⁺. For each cation, the binding affinity difference between binding with the 1a/5e and 5a/1e conformations decreases with the increase of cation radii with values of 9.80, 3.56, and 1.36 kcal/mol respectively for Li⁺, Na⁺ and K⁺.

For the alkali cation complexes, the M⁺-Ins(2)P₁⁰(1a/5e) complexes have lower total energies than the M⁺-Ins(2)P₁⁰(5a/1e) complexes. The relative stability between the two chair forms of the cation complexes (M⁺-Ins(2)P₁⁰(1a/5e) vs M⁺-Ins(2)P₁⁰(5a/1e)) drops to 3.00, 3.25, and 5.44 kcal/mol for the Li⁺, Na⁺, and K⁺ ion complexes correspondingly from 7.56

kcal/mol for bare Ins(2)P₁⁰. This is probably due to the extra stability induced by the higher binding energies of the alkali cations with the 5a/1e conformation. For Li⁺, Na⁺, to K⁺ in that order, the energy difference between two chair conformations of the complexes approaches that for bare Ins(2)P₁⁰ due to longer coordination bonds and weaker interactions with the intra-HBN.

In general, the divalent cations bind to Ins(2)P₁⁰ with approximately four times the binding energies of the monovalent cations because their larger charges result in larger ion-dipole interactions. The strength of the ion-dipole interactions should correlate with the magnitude of the dipole moments of Ins(2)-P₁⁰. Ca²⁺ binds with lower free energy gain than Mg²⁺,³⁸⁻⁴¹ These calculations predict that the binding energy for Mg²⁺ is about 50% higher than for Ca²⁺ in the M²⁺-Ins(2)P₁⁰ complexes (1a/5e and 5a/1e). Both Mg²⁺ and Ca²⁺ bind to Ins(2)-P₁⁰(5a/1e) somewhat more strongly than to Ins(2)P₁⁰(1a/5e) because the M²⁺-Ins(2)P₁⁰(5a/1e) complexes have one more M²⁺-O coordination bond. Similar to the alkali cations, the binding energy difference between the two chair conformation complexes is predicted to decrease from 3.38 kcal/mol for Mg²⁺-Ins(2)P₁⁰ to 0.25 kcal/mol for Ca²⁺-Ins(2)P₁⁰. The dominate conformation for the divalent cation complexes is the

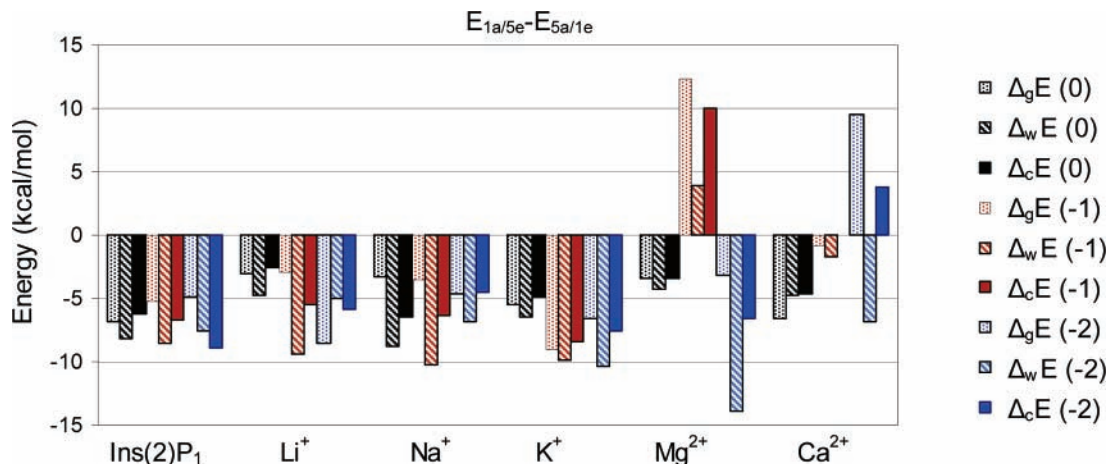


Figure 3. Energies difference between ($E_{1a/5e} - E_{5a/1e}$) conformations.

1a/5e conformation with energy differences of -3.42 and -6.56 kcal/mol for Mg^{2+} and Ca^{2+} , respectively.

2.2. $M^{n+}-Ins(2)P_1^{1-}$. The binding energy of $M^{n+}-Ins(2)P_1^{1-}$ is predicted to be much higher than for the corresponding complexes $M^{n+}-Ins(2)P_1^0$ due to stronger ion-ion interactions involving the negatively charged deprotonated phosphate group. But similar to $Ins(2)P_1^0$, the binding order is $Mg^{2+} > Ca^{2+} > Li^+ > Na^+ > K^+$ for both the 1a/5e and 5a/1e conformations. These calculations predict that for the complexes with $Ins(2)P_1^{1-}(1a/5e)$, the binding energy for Li^+ is about 18% higher than that for Na^+ and the binding energy for Na^+ is about 15% higher than that for K^+ . These numbers change to 19% and 21% for the complexes with $Ins(2)P_1^{1-}(5a/1e)$. For each of the alkali cation complexes, $M^+-Ins(2)P_1^{1-}(1a/5e)$ and $M^+-Ins(2)P_1^{1-}(5a/1e)$, the 1a/5e conformation complex is more stable. The energy difference between the complexes of the two chair forms are 2.98, 3.52, and 9.05 kcal/mol respectively for Li^+ , Na^+ , and K^+ , compared to the energy difference 6.17 kcal/mol between the two chair forms of bare $Ins(2)P_1^{1-}$.

Except for K^+ , the binding energies for most cations are higher for the 5a/1e form than for the 1a/5e form. These model calculations predict that the binding energy for the Mg^{2+} cation with the 5a/1e conformation is 17.67 kcal/mol higher than for the 1a/5e conformation. Consequently, the $Mg^{2+}-Ins(2)P_1^{1-}(5a/1e)$ complex is more stable than the $Mg^{2+}-Ins(2)P_1^{1-}(1a/5e)$ complex by 12.36 kcal/mol even though $Ins(2)P_1^{1-}(5a/1e)$ is less stable than $Ins(2)P_1^{1-}(1a/5e)$ by 6.17 kcal/mol. This is because an additional $Mg^{2+}-O$ coordination bond is formed within $Mg^{2+}-Ins(2)P_1^{1-}(5a/1e)$; Mg^{2+} is tetradentated rather than tridentated as in $Mg^{2+}-Ins(2)P_1^{1-}(1a/5e)$. As a result, the dominant conformation changed from 1a/5e to 5a/1e for the complex of $Ins(2)P_1^{1-}$ with the Mg^{2+} cation. Similar analysis shows that the binding energy of Ca^{2+} is higher for $Ins(2)P_1^{1-}(5a/1e)$ than for $Ins(2)P_1^{1-}(1a/5e)$ by 4.43 kcal/mol. Therefore, the two chair forms complexes with Ca^{2+} have almost the same energy (0.88 kcal/mol difference) due to the formation of one more $Ca^{2+}-O$ coordination bond and fewer hydrogen bonds in the $Ca^{2+}-Ins(2)P_1^{1-}(5a/1e)$ complex.

This data indicates that a chair conformation inversion could happen during the deprotonation process from $Ins(2)P_1^0$ to $Ins(2)P_1^{1-}$ in the presence of the alkaline earth cations, as shown in Figure 3. Consequently, this conformational change may generate a signal for transduction. It should be pointed out here that this interaction, as mentioned previously, involves direct binding between the cations and $Ins(2)P_1$ which raises the question as to whether the same phenomena would be observed with the fully solvated cations having stable solvation shells.

2.3. $M^{n+}-Ins(2)P_1^{2-}$. As expected, the binding energy of $M^{n+}-Ins(2)P_1^{2-}$ is predicted to be much higher than for the corresponding complexes $M^{n+}-Ins(2)P_1^0$ and $M^{n+}-Ins(2)P_1^{1-}$, with the same binding order for both chair conformations: $Mg^{2+} > Ca^{2+} > Li^+ > Na^+ > K^+$.

The binding energy for Li^+ is about 16% higher than for Na^+ and Na^+ is about 12% higher than for K^+ with $Ins(2)P_1^{2-}(1a/5e)$. The corresponding numbers are 15% and 13% with $Ins(2)P_1^{2-}(5a/1e)$. For each alkali complex, the 1a/5e conformation of $M^+-Ins(2)P_1^{2-}$ is more stable than 5a/1e conformation of $M^+-Ins(2)P_1^{2-}$ based upon the stronger binding to the 1a/5e conformation.

The $M^{2+}-Ins(2)P_1^{2-}$ binding energies are the highest among all systems studied. And these systems are stabilized by the enhanced hydrogen-bonding network within both chair conformations. But the relative stability of the two chair conformations has changed. Before combining with the calcium ion, the dominate chair form for bare $Ins(2)P_1^{2-}$ is the 1a/5e conformation which is 4.56 kcal/mol lower than the corresponding 5a/1e chair form. For Mg^{2+} , the binding energy with $Ins(2)P_1^{2-}(5a/1e)$ is slightly higher than that with $Ins(2)P_1^{2-}(1a/5e)$ by 1.71 kcal/mol. Combined with the energy difference between the two chair forms of bare $Ins(2)P_1^{2-}$, the $Mg^{2+}-Ins(2)P_1^{2-}(1a/5e)$ is the stable structure. Since Ca^{2+} binds to $Ins(2)P_1^{2-}(5a/1e)$ with a much higher energy (14.41 kcal/mol) than to $Ins(2)P_1^{2-}(1a/5e)$, the 5a/1e conformation of the complex has a lower energy by 9.49 kcal/mol in the gas phase. However, the relative stability depends on the environment as shown in Figure 3, which will be discussed in next section. As a consequence, during the deprotonation process from $Ins(2)P_1^0 \rightarrow Ins(2)P_1^{1-} \rightarrow Ins(2)P_1^{2-}$, the calcium ions could cause a conformation change (1a/5e \rightarrow 5a/1e) and thus when in a low dielectric environment induce a signal transduction.

Examination of the Mulliken charges retained by the alkali metal ion in these complexes shows that, for the $M^+-Ins(2)P_1$ complexes, Li^+ retains less charge (0.37~0.75e) than Na^+ (0.77~0.96e) and K^+ (0.86~0.96e). For the $M^{2+}-Ins(2)P_1$ systems, Mg^{2+} (0.70~1.25e) retains less charges than Ca^{2+} (1.5~1.73e). These results confirm the electrostatic nature of the bonding but also demonstrate that there is some covalent component in the $M^{n+}-Ins(2)P_1$ interactions, especially in the Li^+ and Mg^{2+} systems. This result is consistent with the polarizing power (z/r^2) of metal cations, where z is the charge of cation and r is the ionic radii respectively. In these systems, the shorter Li^+-O and $Mg^{2+}-O$ bond distances allow the metal ion to more effectively withdraw electron density from the coordinating oxygen atoms on $Ins(2)P_1$, thus reducing the charge

retained by the metal ion. This in turn causes more perturbation to the cooperative HBN centered on the cyclohexane ring.

The ZPE corrections for these complexes could be neglected since their net contributions are very small. A comparison of ΔE_{BE} and ΔG_{BE} in Table 2 reveals that the binding for all of these metal cations are energy driven and thermodynamically favorable even though ΔS_{BE} is always negative as expected (ΔG_{BE} is always negative but has smaller absolute value than ΔE_{BE}).

3. Solvation Effects. The dielectric properties of the environment plays an important role in the process of the metal cations binding to Ins(2)P₁. The predicted free energies and binding energies for metal cations binding to inositol phosphate are listed in Table 2. We studied the gas phase ($\epsilon = 1$), protein encapsulated sites as characterized by an approximate dielectric constant ($\epsilon = 4.9$ for chloroform, CHCl₃), and fully solvent-accessible sites, i.e., aqueous solution, ($\epsilon = 78.39$).

In the gas phase, the binding reactions could happen with high free energy decrease resulting in high binding energies. This is due to the strong attractive Coulombic interactions between the oppositely charged metal cations and the phosphate group. With the increase of the dielectric constant for the solvent, the magnitude of the binding energy for each cation with both chair forms of Ins(2)P₁ decreases significantly. The Gibbs free binding energy in the gas-phase could be more than 10 times larger in magnitude than in a polar solvent such as water, which has larger effects than a nonpolar solvent. For all of the cations studied here (Li⁺, Na⁺, K⁺, Mg²⁺ and Ca²⁺), their complexes with Ins(2)P₁⁰, Ins(2)P₁¹⁻ and Ins(2)P₁²⁻ all have binding energies in the following order:

$$\Delta_g E_{BE}(M^{n+} - \text{Ins}(2)\text{P}) > \Delta_{\text{CHCl}_3} E_{BE}(M^{n+} - \text{Ins}(2)\text{P}) > \Delta_{\text{Water}} E_{BE}(M^{n+} - \text{Ins}(2)\text{P})$$

$$n = 1, 2$$

A low-dielectric cavity enhances the electrostatic interactions between the metal cations and the oxygen atoms in the phosphate group and its vicinal hydroxyl groups. As a result, those metal cations thermodynamically prefer inner-sphere binding over the outer-sphere complexes. In a solvent-exposed environment with a high dielectric constant, the binding occurs with much smaller binding energies by the reason of the high hydration effect between cations and solvent molecules resulting in a diminution of the direct electrostatic and ion-dipole interactions. Normally, the polar solvent induces a bigger entropy component than a nonpolar solvent, as shown in Table 2 by the difference between the ΔE_{BE} and the corresponding ΔG_{BE} .

For each deprotonation state of Ins(2)P₁, the effects of solvation on the complex are in the order of Li⁺ < Na⁺ < K⁺ and Mg²⁺ < Ca²⁺. Because of the comparatively stronger binding and relatively smaller volume of the Li⁺ and Mg²⁺ complexes, they are affected least by the solvent molecules.

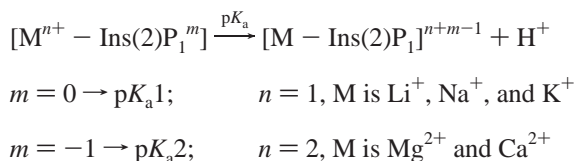
The solvent can affect the thermodynamically preferred conformation of the Ca²⁺-Ins(2)P₁²⁻ complex. In the gas-phase, the 5a/1e conformation complex is more stable with a free energy difference 9.49 kcal/mol as discussed above. If the complex is buried inside a protein, the conformation preference is still 5a/1e but with a much smaller value of 3.77 kcal/mol. But when the complex is surrounded by water, the conformation preference returns to 1a/5e with a relatively large free energy difference of 6.77 kcal/mol. That means that essentially all (>99.9%) of these molecules go through a chair inversion if the environment is changed from a nonpolar environment to an

aqueous environment. This strong coupling between the conformational change and the environment is of fundamental importance for biological processes.

Due to the insolubility of Ins(2)P₁ in a nonpolar solvent at any deprotonation state, no experimental observation is available to compare to the solvent dependence predicted here. It is extremely hard to design experiments to investigate solvent dependent properties and avoid the solvation shell effects of metal cations at same time. Carefully designed experimental verification of these results for the Mg²⁺ and Ca²⁺ is needed, because the simple aqueous solution brings in many other unavoidable interactions which can dramatically affect the direct interactions between the cations and hydrogen-bonding network. Although microwave (MW) spectroscopy and gas electron diffraction (GED) could be used to measure intramolecular hydrogen bonds at low pressure, it is very difficult to detect the interactions within a one-to-one pair of a cation and a hydrogen-bonding system. Under such circumstance, theoretical calculation is the best option to identify these subtle interactions. The continuum method used here gives the direct interactions between the cation and phosphate group with none of the intervening water molecules usually associated with the hydrated cation. In order to accurately reproduce the behavior of the complexes in water or other molecular solvents, the next step will be to explicitly include the hydration shell along with the PCM procedure for all of the systems studied here. Molecular dynamics calculations would help to understand the pathway of binding including the displacement of the metal cation solvation shells. However this requires ab initio molecular dynamics or a force field which can accurately reproduce the interactions between hydrogen bonds and cations.

4. pK_a for Complexes. The instantaneous pK_a of a given group is influenced by its electronic environment, which is determined by its conformation, state of deprotonation and counterions. pK_a prediction is still an issue for biomolecular simulations because there are multiple sites that can deprotonate or protonate.⁴²⁻⁴⁴ An additional complexity can arise when mobile counterions are added that cause more complicated interactions and conformational changes.

When calculating the pK_a, we assume that the chair conformation of the complexes remain unchanged upon deprotonation. Even with the possibility that deprotonation may change the relative stability of the conformations, we assume that the conformation is not changed during the process of deprotonation because the deprotonation process is much faster than the more complex multistep ring inversion. The pK_a is defined by the following:



As shown by the calculated data in Table 4, the presence of the metal cation assists the deprotonation of Ins(2)P₁ by giving a smaller pK_a than that for the uncomplexed Ins(2)P₁. Since the cations stabilized the charge on the deprotonated phosphate group, the values for pK_a1 decrease from 0.36 to -0.44, -0.47, and -0.35, respectively, for Li⁺, Na⁺ and K⁺, and to -1.83 and -1.39, respectively, for Mg²⁺ and Ca²⁺.

In a similar fashion, cations also increase the dissociation of the second proton by compensating the increase in the negative charge that results from the second deprotonation. In the same

TABLE 4: pK_a Values of Ins(2)P₁

	M ⁿ⁺ -Ins(2)P ₁ ⁰ → M ⁿ⁺ -Ins(2)P ₁ ¹⁻ (pK _{a1})		M ⁿ⁺ -Ins(2)P ₁ ¹⁻ → M ⁿ⁺ -Ins(2)P ₁ ²⁻ (pK _{a2})	
	1a/5e	5a/1e	1a/5e	5a/1e
Ins(2)P	0.36	0.37	4.17	7.09
Li ⁺ -Ins(2)P	-0.44	0.34	3.26	1.88
Na ⁺ -Ins(2)P	-0.47	-0.08	3.48	2.03
K ⁺ -Ins(2)P	-0.35	0.38	3.47	2.51
Mg ²⁺ -Ins(2)P	-1.83	-3.22	1.46	4.05 ^a
Ca ²⁺ -Ins(2)P	-1.39	-1.85	3.42	3.67

^a The predicted pK_a is 4.05 since the 5a/1e conformation is predicted to be more stable.

order, the pK_{a2} for the alkali ion complexes are 3.26, 3.48 and 3.47 which are smaller than the value of 4.17 for the bare Ins(2)P₁¹⁻. A notable point that needs to be mentioned is that the pK_{a2} for the Mg²⁺ complex is not 1.46 but 4.05 due to the higher stability of the 5a/1e conformation over the 1a/5e conformation of the Mg²⁺-Ins(2)P₁¹⁻ complex. The pK_{a2} calculation should be calculated based on the more stable 5a/1e conformation. The pK_{a2} for the Ca²⁺ complex is between 3.42 and 3.67 due to the almost equal distribution of the two chair forms. This observation tells us that the interactions with counterions and the induced conformational changes upon protonation or deprotonation must be modeled accurately in order to predict correct pK_a values. Our calculations show that the predicted 5a/1e conformation gave a much more reasonable pK_a value of 4.05 versus a value of 1.46 for the 1a/5e conformation predicted by the NMR data. However, these high level quantum mechanical results can provide guidance for performing reliable molecular mechanics/molecular dynamics simulations on larger more complete systems.

5. Conclusions

This paper primarily focuses on theoretical research aimed at probing subtle perturbations of metals and phosphate groups on the hydrogen-bonding networks in model systems composed of phosphate and hydroxyl groups in various medium/ environments. More specifically, we presented here a density functional theory investigations of the influences from metal cations on the pattern and electronic structure of the intramolecular hydrogen-bonding network in *myo*-inositol 2-monophosphate in the gas phase, aqueous solution and chloroform. The last mimics the environment of protein interiors. The present results reveal a strong coupling between the conformational preference of these components and the interactions with metal ions, the environmental pH, and the dielectric strength of the surrounding medium. This could lead to a better understanding of the physiological role of metals in biology.

The dominate interaction is the electrostatic attraction between cations and the charged phosphate group. Smaller cations tightly bind to the 1a/5e and 1e/5a chair conformations with larger affinities. Generally speaking, for any conformation of Ins(2)-P₁, the binding order for cations is Mg²⁺ > Ca²⁺ > Li⁺ > Na⁺ > K⁺. The coordination bonds with small cations, i.e., Li⁺ and Mg²⁺, have appreciable covalent character. Except for the monodentate bond between the alkali cations and the 1a/5e conformation of Ins(2)P₁⁰, all other combinations prefer a multidentate bonding pattern between the cations and Ins(2)P₁. The more negative the charge on the phosphate group, i.e., the higher degree of deprotonation, the more the metal cation is trapped or localized by the phosphate group. The thermodynamic analysis shows that the ZPE corrections are small and can be

neglected. The metal cation binding process is driven by the enthalpy gain rather than the entropic contribution.

Of all the cations studied here, the divalent alkaline earth metal ions, Mg²⁺ and Ca²⁺, stand out as showing exceptional behavior. The conformational preference for metal binding is pH dependent and solvent dependent. For example, Mg²⁺-Ins(2)P₁⁰ and Mg²⁺-Ins(2)P₁²⁻ favor the 1a/5e form while Mg²⁺-Ins(2)P₁¹⁻ favors the 5a/1e conformation. The Ca²⁺-Ins(2)P₁²⁻ complex prefers the 5a/1e conformation in the gas phase and protein environment, which inverts to the 1a/5e conformation upon entering the aqueous phase. This may help explain the unique biological role that these cations play in signal transduction.

Acknowledgment. This work was supported by the National Science Foundation under the following NSF program: Partnerships for Advanced Computational Infrastructure, Distributed Terascale Facility (DTF), and Terascale Extensions: Enhancements to the Extensible Terascale Facility, (grant number TG-CHE040041N).

Supporting Information Available: The coordinates of the optimized Mⁿ⁺-Ins(2)P₁ complexes and the full reference for Gaussian03 (ref 37) are available free of charge via the Internet at <http://pubs.acs.org>.

References and Notes

- (1) In *Metal Ions in Biological Systems*; Sigel, A., Sigel, H., Eds.; Marcel Dekker: New York, 1996; Vol. 32.
- (2) Catterall, W. A. *Science* **1988**, *242*, 50.
- (3) Fisher, S. K.; Novak, J. E.; Agranoff, B. W. *J. Neurochem.* **2002**, *82*, 736.
- (4) Saenger, W. *Principles of Nucleic Acids Structure*; Springer-Verlag: Berlin, 1984.
- (5) Nakano, S. I.; Fujimoto, M.; Hara, H.; Sugimoto, N. *Nucl. Acid. Res.* **1999**, *27*, 2957.
- (6) Bock, C. W.; Katz, A. K.; Markham, G. D.; Glusker, J. P. *J. Am. Chem. Soc.* **1999**, *121*, 7360.
- (7) Blank, G. E.; Pletcher, J.; Sax, M. *Acta Crystallogr., Sect. B* **1975**, *31*, 2584.
- (8) Gill, R.; Mohammed, F.; Badyal, R.; Coates, L.; Erskine, P.; Thompson, D.; Cooper, J.; Gore, M.; Wood, S. *Acta Crystallogr., Sect. D* **2005**, *61*, 545.
- (9) Yang, P.; Murthy, P. P. N.; Brown, R. E. *J. Am. Chem. Soc.* **2005**, *127*, 15848.
- (10) Agranoff, B. W.; Fisher, S. K. *Psychopharmacol. Bull.* **2001**, *35*, 5.
- (11) De Freitas, D. M.; Castro, M. M. C. A.; Gerald, C. F. G. C. *Acc. Chem. Res.* **2006**, *39*.
- (12) Toker, A. *Cell. Mol. Life Sci.* **2002**, *59*, 761.
- (13) Irvine, R. F.; Schell, M. J. *Nat. Rev. Mol. Cell. Biol.* **2001**, *2*, 327.
- (14) Alam, T. M. *Ab Initio Calculation of Nuclear Magnetic Resonance Chemical Shift Anisotropy*; Sandia National Laboratories, 1998.
- (15) Becke, A. D. *Phys. Rev. A: At., Mol. Opt. Phys.* **1988**, *37*, 785.
- (16) Becke, A. D. *J. Chem. Phys. A* **1993**, *98*, 5648.
- (17) Lee, C.; Yang, W.; Parr, R. G. *Phys. Rev. B* **1988**, *37*, 785.
- (18) Pavlov, M.; Siegbahn, P. E. M.; Sandstrom, M. *J. Phys. Chem. A* **1998**, *102*, 219.
- (19) Dudev, T.; Cowan, J. A.; Lim, C. J. *Am. Chem. Soc.* **1999**, *121*, 7665.
- (20) Katz, A. K.; Glusker, J. P.; Beebe, S. A.; Bock, C. W. *J. Am. Chem. Soc.* **1996**, *118*, 5752.
- (21) Cheeseman, J. R.; Frisch, M. J.; Devlin, F. J.; Stephens, P. J. *Chem. Phys. Lett.* **1996**, *252*, 211.
- (22) Barrientos, L. G.; Murthy, P. P. N. *Carbohydr. Res.* **1996**, *296*, 36.
- (23) Volkmann, C. J.; Chateaufneuf, G. M.; Pradhan, J.; Bauman, A. T.; Brown, R. E.; Murthy, P. P. N. *Tetrahedron Lett.* **2002**, *43*, 4853.
- (24) Miertus, S.; Scrocco, E.; Tomasi, J. *Chem. Phys.* **1981**, *55*, 117.
- (25) Cossi, M.; Barone, V.; Cammi, R.; Tomasi, J. *Chem. Phys. Lett.* **1996**, *255*, 327.
- (26) Barone, V.; Cossi, M.; Mennucci, B.; Tomasi, J. *J. Chem. Phys. A* **1997**, *107*, 3210.
- (27) Cancès, M. T.; Mennucci, B.; Tomasi, J. *J. Chem. Phys. A* **1997**, *107*, 3032.

- (28) Barone, V.; Cossi, M.; Tomasi, J. *J. Comput. Chem.* **1998**, *19*, 404.
- (29) Wong, S. E.; Bernacki, K.; Jacobson, M. *J. Phys. Chem. B* **2005**, *109*, 5249.
- (30) Tomasi, J. *Theor. Chem. Acc.* **2004**, *112*, 184.
- (31) Gilson, M. K.; Honig, B. H. *Biopolymers* **1986**, *25*, 2097.
- (32) Chipman, D. M. *J. Phys. Chem. A* **2002**, *106*, 7413.
- (33) Klicic, J. J.; Friesner, R. A.; Liu, S. Y.; Guida, W. C. *J. Phys. Chem. A* **2002**, *106*, 1327.
- (34) Richardson, W. H.; Peng, C.; Bashford, D.; Noodleman, L.; Case, D. A. *Int. J. Quantum Chem.* **1997**, *61*, 207.
- (35) Cammi, R.; Mennucci, B.; Tomasi, J. *J. Phys. Chem. A* **2000**, *104*, 5631.
- (36) Cammi, R.; Mennucci, B.; Tomasi, J. *J. Phys. Chem. A* **1999**, *103*, 9100.
- (37) Frisch, M. J., et al. Gaussian 2003 Pittsburgh PA, 2003.
- (38) Garmer, D. R.; Gresh, N. *J. Am. Chem. Soc.* **1994**, *116*, 3556.
- (39) Gresh, N.; Garmer, D. R. *J. Phys. Chem.* **1996**, *100*, 4790.
- (40) Bock, C. W.; Katz, A. K.; Markham, G. D.; Glusker, J. P. *J. Am. Chem. Soc.* **1999**, *121*, 7360.
- (41) Dudev, T.; Lim, C. *J. Phys. Chem. B* **2000**, *104*, 3692.
- (42) Mongan, J.; Case, D. A. *Curr. Opin. Struct. Biol.* **2005**, *15*, 157.
- (43) Figueirido, F.; Del, Buono, G. S.; Levy, R. M. *J. Phys. Chem.* **1996**, *100*, 6389.
- (44) Simonson, T.; Carlsson, J.; Case, D. A. *J. Am. Chem. Soc.* **2004**, *126*, 4167.